Published in final edited form as:
Biochemistry. 2013 November 19; 52(46): 8237–8245. doi:10.1021/bi401376u.

Novel heparin-binding motif in decorin binding protein A from strain B31 of *Borrelia burgdorferi* explains higher binding affinity

Ashli Morgan and **Xu Wang**
Department of Chemistry & Biochemistry, Arizona State University, Tempe, AZ 85287

Abstract

Decorin-binding protein A (DBPA), a glycosaminoglycan (GAG) binding lipoprotein found in *Borrelia burgdorferi*, is crucial to the transmission of Lyme disease in its earliest stages. Due to its role in the initial transmission of the disease, DBPA is an ideal target for vaccine development. DBPA sequences from different strains also contain considerable heterogeneity, leading to differing affinities for GAGs and proteoglycans among different DBPA sequences. Through biophysical and structural analysis of DBPA from the strain B31, we have discovered a novel and important GAG-binding epitope in B31 DBPA. Removal of the epitope greatly attenuated its affinity for DBPA and may explain the differential GAG affinities seen in DBPAs from other strains of Borrelia burgdorferi. Paramagnetic perturbation of the protein with TEMPO-labeled heparin fragments showed bound GAGs are located close to the linker region containing the BXBB motif plays a significant role in determining affinity and orientation of GAG-binding to DBPA is specific. Thermodynamic contributions of the new motif to GAG binding was also characterized with both NMR and ITC and compared with other DBPA residues previously known to be involved in GAG interactions. These analyses showed the motif is as important as other known binding epitopes. The discovery of the motif offers a possible structural explanation to the previous observed differences in GAG affinities of DBPA variants from different *Borrelia* strains and increases our understanding of DBPA-GAG interactions.

Keywords

glycosaminoglycan; bacterial adhesin; GAG-protein interactions; solution NMR; paramagnetic GAG ligand

Pathogens often employ surface polysaccharides on host cells as receptors for their initial contacts. Many of them prefer the sulfated polysaccharide glycosaminoglycan (GAG) as their target. So far, GAGs have been shown to be the target of a number of microbes and viruses, including *Mycobacterium tuberculosis*, *Streptococcus agalactiae*, *Plasmodium falciparum* and herpes simplex virus. These pathogens interact with GAGs through GAG-binding surface proteins, and disruption of these interactions often have an adverse effect on the dissemination of the pathogens and constitute a new path for therapeutic treatment of infectious diseases. Among the microbes known to bind GAGs is the bacterium *Borrelia burgdorferi*, the causative agent of Lyme disease. Lyme disease is a common vector-borne

Corresponding Author: Xu Wang, Department of Chemistry & Biochemistry, Arizona State University, Tempe, AZ 85287, USA. xuwang@asu.edu. Phone:480-7278256.

SUPPORTING INFORMATION

SDS-PAGE analysis of sample purity, GMSA analysis of DS d6-DBPA interaction, scheme for reductive amination of heparin fragments, fittings of K_Ds for heparin-DBPA interactions, ITC titrations of DBPAs with heparin dp6 and multi-sequence alignment of DBPAs from different strains of *Borrelia burgdorferi* are included in the supporting information. This material is available free of charge via the Internet at http://pubs.acs.org.

illness that can result in symptoms ranging from minor skin rashes to more serious joint, heart, and neural diseases if not treated. Ticks infected with *Borrelia burgdorferi* transmit the bacterium into the host through bites, and the bacterium colonizes the extracellular matrix (1). *Borrelia* has been shown to have strong interactions with the matrix which allows it to move from the vascular system into the surrounding tissues. The spread of the bacterium outside of the vascular system is often a requirement for the advanced stages of the disease and is not easily treated with antibiotics (1–3). Despite the prevalence of Lyme disease, vaccination against this disease has proven to be difficult due to the genetic variability among the many strains of *Borrelia* (1, 4). A potential therapeutic target is decorin-binding protein (DBP). DBP is a surface lipoprotein that is solely expressed during the human infection stage. DBPs were first identified to adhere primarily to decorin, a small proteoglycan found aligned with collagen in connective tissues, but were later shown to have affinity for proteoglycans containing other types of GAG chains (5–8). The importance of the DBP-decorin interaction was demonstrated in studies that showed the absence of either decorin or DBPs decreases the effectiveness of the infection process, especially during its early stages (9–11). Two isoforms of DBP exist in *Borrelia*, commonly referred to as DBPA and DBPB. While both variants are important for infection, DBPA contains greater sequence heterogeneity than DBPB, which makes it a more challenging therapeutic target (10–13).

Both in vivo and in vitro studies have conclusively shown that the GAG segment of decorin is the most biologically relevant binding site for DBPs (5, 14, 15). DBPA, in particular, is known to have affinity with a variety of GAGs. In fact, in vitro studies have revealed that DBPA binds heparin with greater affinity than other GAGs such as dermatan sulfate (DS) or chondroitin sulfate (CS) (7, 14–18). However, DBPA's binding affinity for GAGs seems to differ wildly among different *Borrelia* strains. The most in-depth study of the correlation between DBPA sequence variation and its activity was carried out Benoit et al. (16). They looked at the GAG affinity of strains B31, 297, N40 and B356 from *Borrelia burgdorferi* and strain PBr from *Borrelia garinii* and strain VS461 from *Borrelia afzelii*. It was evident from the binding assays that DBPA from PBr possessed the highest binding affinity for GAGs. This is not surprising because this strain's DBPA contains the highest number of basic amino acids as well as the highest ratio of basic amino acids to acidic amino acids among all strains investigated in the report. However, despite high sequence homology among the four *Borrelia burgdorferi* strains, B31 and 297 versions of DBPAs possessed a much higher affinity for GAGs than N40 and B356 (16). Because of DBPA's role as an extracellular matrix (ECM) adhesin, its GAG binding affinity may be a crucial determinant in *Borrelia* infectivity, making understanding the molecular mechanism underlying its interactions with GAGs a priority. Furthermore, the void in our knowledge of GAG-protein interactions in general means DBPA's sequence-dependent GAG affinity is an excellent opportunity to investigate principles governing GAG-protein interactions. However, there is yet no molecular explanation for the large deviations observed in GAG-binding affinities of DBPAs from four different strains of *Borrelia burgdorferi*.

Attempts to identify GAG-binding epitopes of DBPA started soon after the protein's discovery. Using sequence alignment and a peptide screening approach, Hook and coworkers first identified residues K82, K163 and K170 as critical to the decorin binding ability of DBPA (19). More recently, Benoit et al. serendipitously discovered that the absence of the C-terminus of DBPA from strain VS461 (last 11 to 13 residues of DBPA) abrogated the protein's ability to bind GAGs (16). Unfortunately, because these motifs are shared amongst most strains of *Borrelia burgdorferi*, they do not reveal the structural rationale behind differing GAG affinities between strains B31 and N40. However, the recently solved structure of B31 DBPA does give one clue to the reason behind B31's enhanced GAG affinity: according to the structure, the proposed GAG-binding epitope on

B31 is a basic pocket consisting of helices and two dynamic segments of DBPA. Previously identified GAG-binding motifs are all found in the pocket (Figure 1) (17). Most intriguingly, one of the flexible segments, a linker between helices one and two covering the pocket (residues 58 to 72), contains a BXBB motif (B: basic amino acid) not seen in many versions of DBPA including those from strains N40 and B356.

Guided by the structure for B31, it is now possible to propose a hypothesis explaining the differences in GAG affinities of DBPAs from strains B31 and N40. In particular, we believe the linker BXBB motif maybe of significant importance in promoting DBPA-GAG interactions. In this manuscript, we report the biophysical and structural characterization of the interactions between size-defined GAG fragments and known GAG-binding motifs on B31 DBPA. Our choice of GAG ligands is size-defined low molecular weight heparin. This decision is prompted by the fact that DBPA has very low affinity for low molecular weight DS in vitro, which made accurate characterizations of DBPA's GAG affinity impractical. (20) Heparan sulfates, a form of heparin that resides on epithelial cell surface, are known to act as receptors for Borrelia burgdorferi,(7) and given the promiscuity of most GAG binding proteins, epitopes identified with heparin should be applicable to the binding of other types of GAGs. Through the use of fluorescence-assisted gel mobility shift assays (GMSA), we showed the BXBB cluster in the linker is vital to the GAG affinity of B31 DBPA, such that B31 DBPA's affinity for both low molecular weight heparin and DS decreases significantly in its absence. The free energy contribution of each motif to GAG-binding was also quantitatively characterized using NMR and isothermal titration calorimetry (ITC), and the result correlated well with those observed in gel mobility shift assays. In particular, the linker BXBB motif and the three lysine residues on the helices contributed most to the free energy of binding, and the C-terminal residues contributed much less. ITC results also revealed that the interaction is driven almost entirely by favorable enthalpic changes. The direct interactions of the linker residues with GAGs was confirmed through a NMR paramagnetic relaxation enhancement (PRE) study using a novel TEMPO-tagged paramagnetic heparin ligand. The results unambiguously proved that the linker not only bound heparin but the heparin fragment oriented specifically with the reducing end of the fragment close to the linker. Using observations in the current study, a rationale for the higher GAG affinity seen in B31 DBPA can now be offered along with structural model for the interactions between GAG fragments and B31.

EXPERIMENTAL PROCEDURES

Expression and Purification of B31 variants

ORF for the wildtype mature B31 DBPA (residues 24–191) was synthesized by Genscript Inc. (Piscataway, NJ) and cloned in the pHUE vector which incorporates His-tagged ubiquitin on the N-terminus of B31 to give a fusion protein.(21) Mutagenic primers were designed for four B31 mutants: ^{64}KDKK^{67} to ^{64}SDSS^{67}, ^{176}KKK^{178} to ^{176}SSS^{178}, ^{187}KCK^{189} to ^{187}SCS^{189}, and K82,170S. The forward primers for the mutants were as follows: (^{64}SDSS^{67}) 5′-GCGGTTAACTTCGATGCCTTCAGCGATAGCAGCACCGGCAGTGGTGTGAGCGAAAATCCG-3′, (^{176}SSS^{178}) 5′-CAAAAACTACTGCACGCTGAGCAGCAGCGAAAATAGCACCTTC-3′, (^{187}SCS^{189}) 5′-GCACCTTCACGGATGAAAGCTGTAGCAACAATTGAAAGCTTAG-3′, (K82S) 5′-CCGTTTATCCTGGAAGCCAGCGTGCGTGCAACCACG-3′, and (K170S) 5′-CTGCAGCGCGTGCATACCAGCAACTACTGCACGCTG-3′. Mutagenesis was conducted with the Agilent Quickchange Site-Directed Mutagenesis kit by following the manufacturer's instructions and the incorporation of the mutations was confirmed though sequencing.

To express the protein, plasmid was transformed into *E. coli* BL21(DE3) and the bacteria were grown at 37°C in M9 medium to an OD_{600} of 0.5. The M9 medium was supplemented with $^{15}NH_4Cl$ and/or ^{13}C-glucose depending on the desired isotopic labeling scheme. The bacteria were induced with 0.5 mM IPTG and were incubated overnight at 30°C. The cells were harvested via centrifugation and the resuspended cell pellet was incubated with 1 mg/mL lysozyme then sonicated to lyse the cells. The fusion protein in the supernatant was obtained through Ni-affinity chromatography using a 1 mL HisTrap column (GE Life Sciences). The fusion protein was eluted off the column using an imidazole gradient from 35 mM to 500 mM at a flow rate of 1 mL/min. The fusion protein was exchanged into 25 mM Tris (pH 8.0) and 100 mM NaCl and digested with USP2 and 1 mM DTT overnight at room temperature (21). The cleaved DBPA was purified using a 1 mL HisTrap column. The cleaved DBPA was found in the flow-through, which was collected and concentrated. Supplementary figure 1 shows the SDS-PAGE analysis of the sample during each stage of purification.

Production of Heparin and TEMPO-Labeled Heparin Fragments

Heparin and DS purchased from Sigma Aldrich was first dialyzed and lyophilized to remove excess salt. Porcine mucosa heparin was digested with 0.5IU heparinase I (IBEX Inc.) and DS was digested with Chondroitinase ABC (Sigma Aldrich) until the depolymerization was 30% complete to give short fragments (22). The fragments were separated using a 2.5 cm × 175 cm size exclusion chromatography column (Bio-Rad Biogel P10) with a flow rate of 0.2 mL/min. The fractions containing the same size were pooled, desalted, and lyophilized. No further steps were taken to separate fragments bearing different sulfation patterns. Disaccharide analysis on the fragments used showed that heparin fragments contained ~45 % disulfated disacharrides and ~ 40% trisulfated disaccharides and DS contained mostly monosulfated disaccharides. For the PRE study, the reducing end of heparin hexasaccharide (dp6) fragments was modified using a nitroxide radical, 4-amino-TEMPO, through reductive amination (supplementary figure 2). Specifically, a concentration of 300 μM TEMPO was incubated with 1mg of the heparin fragment and 25 mM $NaCNBH_3$ at 65°C in water for three days. The mixture was then desalted and GAG fragments were isolated using SAX-HPLC.

Gel Mobility Shift Assays for WT B31 and B31 Mutants

Heparin decasaccharides (dp10), heparin hexasaccharides (dp6) and DS hexasaccharides were fluorescently labeled with 0.1 M 2-aminoacridone (2-AMAC).(23) Briefly, 5 μL of 20 mg/mL GAG fragment was mixed with 40 μL of 0.1 M 2-AMAC which had been dissolved in 85% Me_2SO, 15% glacial acetic acid. This mixture was incubated at room temperature for 15 minutes before 40 μL of 1.0 M $NaCNBH_3$ (in deionized water) was added. The fragments were incubated at 37°C overnight and then precipitated by adding 9 volumes of ethanol and incubating the mixture at −20°C for 15 minutes. After centrifugation, the pellet was washed with another 9 volumes of ethanol and the resulting pellet was resuspended in 50 mM sodium phosphate (pH 6.5) and 150 mM NaCl. To perform the gel mobility shift assaysone microgram of the fluorescently labeled heparin fragment was mixed with 0.5, 1, or 2 molar equivalents of WT B31 or B31 mutants in 50 mM sodium phosphate (pH 6.5) and 150 mM NaCl buffer. For the DS dp6 GMSA, the fluorescently labeled fragments were mixed with the protein at a DS-to-protein ratio of 3, and in 50 mM acetate, pH 5 and 150 mM NaCl buffer. The control is the same mixture but with an equal volume of the same buffer without the protein. The reactions were incubated at room temperature for 30 minutes and were run at 120 V for 15–25 minutes in a 1% agarose gel immersed in the same buffer as the buffer used for incubation. A UV panel was used to visualize the shifts (24).

Titrations of WT and Mutant B31 using Heparin dp6

K_D's of the interaction between heparin dp6 and B31 were estimated using NMR monitored titration. Specifically, 2.10 mM of heparin dp6 was added to 400 μL of 150 μM DBPA in 300 μM aliquots. This was done for B31 WT, B31 ^{64}SDSS^{67}, B31 ^{187}SCS^{189} and B31 K82,170S. For B31 ^{176}SSS^{178}, 3.60 mM of heparin dp6 was added to 150 μM DBPA in 600 μM aliquots. The pH of all the protein samples was lowered from pH 6.5 to pH 5.0. A ^{1}H-^{15}N HSQC spectrum was collected at each titration point. The chemical shift changes in the ^{1}H and ^{15}N dimensions were normalized into one chemical shift value. (25) The normalized chemical shift was calculated using the equation $\delta_H = [\Delta\delta_H^2 + (1.7 \times \Delta\delta_N)^2]^{1/2}$ where δ_H and δ_N represent the chemical shifts for ^{1}H and ^{15}N respectively. The K_D of binding was extracted using the fitting feature in xcrvfit (http://www.bionmr.ualberta.ca/bds/software/xcrvfit/) to plot the normalized chemical shift against the ratio of ligand to protein. Data for the titrations were collected on a Bruker Ultra-Shield 600 MHz and 850 MHz spectrometers.

Isothermal Titration Calorimetry of DBPA-heparin Interaction

ITC of DBPA with DBPA with heparin dp6 was performed on a Microcal ITC-200 calorimeter. Samples consisting of 300 μL of 200 μM DBPA were titrated with aliquots of 10 mM heparin dp6 stock solution at 25 C. Buffer containing no protein was used as a reference. Each titration was repeated three times and the average value of the dissociation constant and enthalpy change (ΔH) are reported.

Acquisition and Analysis of Backbone Dynamics Data

All NMR samples consisted of 400 μL of 150 to 200 μM of ^{15}N labeled B31 WT DBPA in 50 mM NaH_2PO_4, pH 6.5 and 150 mM NaCl buffer. NMR data for relaxation spectra were collected on a Bruker Ultra-Shield 600 and Varian Inova 800 MHz spectrometer. Paramagnetic relaxation enhancement (PRE) from TEMPO labeled heparin fragments was quantified by measuring ^{1}H T_2 of the backbone amide protons according to Iwahara et al. (26) before and after the radical on the heparin fragment was reduced with ascorbic acid. The relaxation delays used were 1, 4.5, 8, 11.5, 15 and 18.5 ms. The difference in ^{1}H T_2 before and after reduction of the radical is the relaxation contribution from the TEMPO radical. T_1, T_2, and steady state heteronuclear NOE experiments were collected for B31 WT in the presence and absence of 24 molar equivalents of heparin dp6. The relaxation delays for the T_1 experiments were 0.1, 0.3, 0.5, 0.7, 0.9 and 1.3 second. The relaxation delays for the T_2 experiments were 10, 30, 50 and 70ms. Steady state heteronuclear NOE were derived from peak intensity ratios of spectra collected with and without proton saturation for 3 s. The data were processed with NMRPipe (27) and analyzed using NMRView (28). The order parameter S^2 was extracted using the model-free approach with relax, a model-free software (29). The protein is assumed to undergo isotropic global rotational diffusion and its global rotational correlation time, τ_m, was estimated as the average rotational correlation times of all residues in the structured region. The residue specific correlation times were calculated according to equation 9 from Kay et al. (30), taking into consideration only contributions from J(0) and J(ω_N). In particular, the equation $\tau_C = \frac{1}{4\pi\nu_N}\sqrt{6\frac{T_1}{T_2} - 7}$ was used, where ν_N is the resonance frequency of ^{15}N in Hz. DBPA's internal motions were characterized through the fitting of the parameters S^2 (magnitude of the internal motion), τ_e (internal motion correlation time) and R_{ex} (contribution of conformational exchange to transverse relaxation) for each backbone amide nitrogen atom.

RESULTS

Interaction of B31 mutants with GAGs

To assess the importance of known B31 DBPA GAG-binding motifs to GAG interactions, we created four B31 mutants each lacking a basic amino acid cluster from one of the proposed GAG-binding motifs. The linker mutant ^{64}SDSS^{67} contains the mutations of residues ^{64}KDKK^{67} in the linker to ^{64}SDSS^{67}. The ^{176}SSS^{178} mutant contains the mutations of the C-terminal ^{176}KKK^{178} to ^{176}SSS^{178}. Similarly, ^{187}SCS^{189} mutant contains the mutations of C-terminal residues ^{187}KCK^{189} to ^{187}SCS^{189}. Finally, the K82,170S mutant contains the mutations of two helical residues first identified as being part of the GAG-binding epitope (19, 31). Because native polymers of GAGs induce only signal disappearance when added to samples of DBPA (20), uniform sized fragments of GAGs were used to evaluate mutagenesis-related changes in DBPA's GAG affinity. Furthermore, heparin hexasaccharide (dp6) were chosen as the primary ligand. The choice is a consequence of DBPA's relatively strong affinity for heparin. Similar sized fragments of both DS and CS, the GAG types found on decorin, do not interact strongly with DBPA even under the most optimized conditions (14, 16, 20).

A qualitative characterization of B31-heparin interactions was first conducted with a gel mobility shift assay and fluorescently labeled heparin dp10 fragments (24). The gel mobility shift assay is based on the principle that the migration of the heparin fragments is greatly impeded when proteins are bound. The effect is a combination of an increase in the apparent size of the complex and a reduction in the net charge of the complex. Using such an assay, we measured the GAG affinity of wild type B31 as well as the linker mutant ^{64}SDSS^{67}, the C-terminal mutants ^{176}SSS^{178}, ^{187}SCS^{189}, and the helical mutant K82,170S. The results are shown in Figure 2. The assay clearly demonstrated that B31 WT is capable of inducing shifts in a significant proportion of the heparin fragments. However, the four B31 mutants did not have as great of an effect on heparin fragment migration (Figure 2). ^{64}SDSS^{67} and K82,170S mutants showed no shift of the heparin fragment while ^{176}SSS^{178} and ^{187}SCS^{189} induced minor shifts of the heparin fragment. These observations support the previous studies indicating the importance of lysine residues in binding GAGs. However, the linker BXBB motif and the helical lysine residues contribute more to DBPA B31's GAG affinity than the C-terminal basic clusters. Differences in GAG affinity also exist among the C-terminal clusters. Specifically, the ^{176}SSS^{178} mutant has a larger effect on binding than the ^{187}SCS^{189} mutant. Similar trends were seen with heparin dp6 (supplementary figure 3), although its interactions with the C-terminal mutants of ^{176}SSS^{178} and ^{187}SCS^{189} is not readily visualized as in the heparin dp10, indicating the binding affinity of DBPA for heparin dp6 maybe weaker. The same assay was also carried out with DS dp6 (supplementary figure 4). However, its weak affinity with DBPA demanded the use of conditions more conducive to protein-GAG interactions. In particular, the assay was conducted at pH 5 and at a GAG-to-protein ratio of 3. Under these conditions, some DS binding can be seen for the wild type and the ^{187}SCS^{189} mutant. However, the other three mutants showed no sign of binding DS dp6. This is consistent with what has been observed with heparin fragments, indicating DBPA's interactions with DS and heparin are governed by similar factors.

Thermodynamic contributions of the GAG binding motifs

Titrations were conducted with heparin dp6 on the WT and mutant forms of B31 to quantitatively measure thermodynamic contribution of each motif on GAG binding. Because GAG-protein interactions are highly dependent on the size of the GAG polymer, B31 DBPA's affinity for heparin dp6 is weak at physiological pH (K_D ~ 4 mM). Such weak affinity made detections of affinity changes difficult. As a result the titrations were repeated

at pH 5.0, a pH that produced more favorable electrostatic surface potentials for binding, thus increasing the affinity of DBPA for heparin. Furthermore, the pH change did not change the pattern of peaks or the peak migration direction significantly, indicating DBPA-heparin interactions were not greatly perturbed. With the lower pH, binding of heparin dp6 to B31 WT went from a K_D of 4 mM to 0.5 mM (figure 3). The shifts of two C-terminal residues (E186 and N191) showing the largest migration distances were used to determine the K_D of the interaction for each DBPA variant. The only exception was the mutant K82,170S, for which A54 was used in place of E186 due to the poor signal–to-noise ratio of the E186 peak. Table 1 lists the K_D values derived from N191 and E186 for each B31 variant. It is noteworthy that K_D's obtained using E186 chemical shift migrations are consistently lower than those from N191. This most likely reflects the flexibility of the C-terminus as a binding site and the fact that acidic amino acids are more likely to repel the negatively charged GAG ligands, thus providing a higher K_D. However, these E186-derived K_D's reflect the same trend of decreasing affinities among the mutants examined as N191. Compared to the binding K_D of 0.5 mM for the wild type, the linker mutant ^{64}SDSS^{67} exhibited a much higher K_D. An accurate value of the K_D for the ^{64}SDSS^{67} mutant could not be obtained under the current experimental conditions, but is estimated to be greater than 20 mM. The K_Ds for the helical mutant K82,170S, and the C-terminal mutant ^{176}SSS^{178} and ^{187}SCS^{189} were approximately 4 mM, 2.5 mM and 0.85 mM, respectively. The binding curves for all samples are included in supplementary figure 5. Based on these dissociation constants, the ΔG contributions of the BXBB motif in the linker were calculated to be more than 2.7 kcal/mol while the K82, K170 motif and the C-terminal ^{176}SSS^{178} motif contribute only 1.2 kcal/mol and 1 kcal/mol, respectively. The ^{187}SCS^{189} motif contributes very little thermodynamically to GAG-binding. A summary of the results is presented in Table 1.

To confirm the NMR observations and shed further insight into the thermodynamic driving force of DBPA-GAG interactions, we also performed ITC analysis of the interactions between heparin dp6 and wild type DBPA as well as two weaker binding mutants, ^{64}SDSS^{67} and K82,170S. The ITC results agreed well with the NMR findings. In particular, ITC found the K_D for the complex of wildtype B31 DBPA with heparin dp6 to be ~ 0.8 mM. ITC's estimations on the K_D of heparin dp6's interactions with the ^{64}SDSS^{67} mutant and the K82,170S mutant are less precise because of limitations on the concentrations of both heparin dp6 stock solution, which produced high dilution heat at high concentrations, and the mutants, but both titrations showed clear signs of significant increases in their K_D. The K_D of heparin dp6 interactions with the ^{64}SDSS^{67} mutant is estimated to be ~5 mM. The K_D for the K82,170S mutant is estimated to be around ~ 10 mM (Table 1 and Supplementary Figure 6). These results agree with the trend obtained using GMSA and NMR. Furthermore, similar to other carbohydrate binding proteins (32), DBPA's interaction with heparin dp6 is mostly driven by favorable enthalpic changes, which is estimated at ~ − 4.8 kcal/mol. Entropic changes were small but unfavorable, contributing ~ + 0.5 kcal/mol to the free energy change. Supplementary figure 6 shows the ITC titration curve of the wild type as well as ^{64}SDSS^{67} and K82,170S mutants with heparin dp6.

Specific DBPA-GAG interactions using paramagnetic-labeled GAG ligands

In our previous characterization of B31 DBPA structure, indirect indications of the flexible linker's role in contacting GAGs were already evident. In particular, NMR chemical shifts of atoms in linker residues underwent significantly larger changes than residues in other parts of the protein, and amide protons of residues G69, S70 and G71 saw dramatic decreases in solvent exchange rates in the presence of heparin dp6.(20) To obtain direct evidence that the linker is close to the bound GAG, we probed B31 DBPA with a novel paramagnetic heparin dp6 ligand. The paramagnetic functional group used in this study is TEMPO, a stable nitroxide radical that has commonly been used as a structural probe in

solution NMR. The paramagnetic effect of TEMPO stems from the unpaired electron that generates an inhomogeneous magnetic field in its vicinity, causing NMR signals of nearby atoms to experience larger longitudinal and transverse relaxation rates, leading to signal broadening. Such an effect is referred to paramagnetic relaxation enhancement (PRE). Since PRE is distance dependent, the residues closest to the radical will experience greatest increases in relaxation rates, which can be quantitatively measured.(26) TEMPO tagged glycans have been used to probe protein-glycan interactions before (33, 34). However, there is no report of location specific TEMPO-labeling of GAG fragments for the purpose of studying protein-GAG interactions. For this study, we constructed a novel TEMPO-labeled heparin dp6 derivative by attaching 4-amino-TEMPO specifically to the reducing end of the heparin dp6 fragment using reductive amination (supplementary figure 2). Although reductive amination has been used to attach fluorescent tags to heparin, this is the first report of stable radical functionalization of heparin using reductive amination. To accurately quantify the size of the PRE on each residue, the amide proton transverse relaxation rates were measured in the presence of six molar equivalents of TEMPO-labeled heparin dp6 before and after reducing the TEMPO radical with ascorbic acid. The difference in the two relaxation rates is due entirely to the PRE from the nearby radical. This allowed the location of the reducing end of heparin to be accurately determined. Figure 4a shows the residue specific PRE of each backbone amide proton. The residues that showed the most perturbation after the radical was reduced were N59 and F60, both of which showed a rate decrease of more than 20 s^{-1}. Supplementary figure 7 shows the HSQC peaks of the two residues in the presence of oxidized and reduced radical as well as the normalized intensity decay curve from which the relaxation rates were calculated. These residues are positioned at the N-terminal end of the linker and close to the BXBB motif. Their perturbation indicates the radical was positioned near the BXBB epitope in the linker. Because the radical was specifically attached to the reducing end of the heparin fragment, the PRE data imply that the reducing end of the fragment is present near the BXBB epitope as well. These data provide direct confirmation that the BXBB motif is part of the GAG binding site of DBPA. It is also noteworthy that other basic amino acid clusters in the protein showed minimal perturbation by the TEMPO-labeled heparin. However, this may be because these residues only interact with regions of heparin distant from the reducing end. To confirm the PRE effect is not the result of non-specific TEMPO-DBPA interactions, the protein was also titrated with 4-amino-TEMPO at similar protein-to-ligand ratios, and no significant changes in the transverse relaxation rates of the protein were observed.

Backbone Dynamics of B31 DBPA

Because both the linker and the C-terminus of DBPA are quite flexible, the possibility of GAG-induced changes in backbone dynamics of the protein exists. To quantify these changes, the popular Model-Free approach was used to estimate the extent of ps to ns time scale internal motions in the protein (35, 36). This technique allowed the magnitude of internal motions of the atoms to be represented by the simple order parameter S^2. Furthermore, its value can be estimated using measureable NMR observables such as longitudinal and transverse relaxation rates and steady state heteronuclear NOE (30). These observables were measured on the backbone amide nitrogen atom using established NMR experiments, and the experimental data were fitted using the software relax (29) to obtain residue-specific order parameters. The fitting assumes the protein undergoes isotropic global rotational motion, which is usually true for well folded globular proteins. To perform the fitting, global rotational correlation time (τ_m) of the protein were estimated using transverse and longitudinal relaxation rates of residues located in the structured parts of the protein. In the absence of heparin dp6, τ_m was estimated to be ~ 12.5 ns. After 24 equivalents of heparin dp6 has been added, τ_m increased slightly to 14.2 ns. Figure 5 shows the order parameters of backbone amide nitrogen atoms of B31 WT in the presence and absence of 24

equivalence of heparin dp6. An order parameter value of 0 indicates a complete lack of internal order while a value of 1 indicates the atom is perfectly rigid relative to other atoms and experiences no internal motion. The values of order parameters for the structured parts of the protein are around 0.85 (Figure 5). No large changes in order parameter were observed for the heparin containing sample. However, some reductions in order parameters were observed for residues in the first half of the linker. In particular, residue F60, which is one of two residues greatly perturbed by the paramagnetic ligand, showed an increase of ~ 0.15 in its S^2 value after heparin dp6 was added. These measurements indicate presence of heparin dp6 did not change the magnitudes of DBPA's fast time scale motions significantly. The lack of large scale changes in protein dynamics is consistent with ITC measurements, which showed entropic contributions to binding are small. To ensure the accuracy of the fitting, contributions to observed relaxation rates from μs - ms time scale conformational exchange (R_{ex}) was also estimated in the model. However, no significant contributions from motions at this time scales were seen.

DISCUSSION

Since their discovery, DBPA's role in the development of Lyme disease has been extensively studied (10–12, 37). It has been shown to be important in the establishment of infection at early stages of the process and may act by both anchoring bacteria to the extracellular matrix and modulating the immune system response to the bacterium (11). One aspect of DBPA's activity that has not been fully explored is the relationship between variations in its sequences and its activity as an adhesin. In particular, a previous study revealed that DBPAs from strains B31 and 297 of *Borrelia burgdorferi* possessed much higher GAG affinity than strains N40 and B356 despite a high sequence homology among them.(16) Our results offer a possible explanation for the observations: both B31 and 297 DBPAs contain the BXBB motif in the linker, where as in N40 and B356 the motif is substituted with the sequence TDSE (supplementary figure 8), making the net charge for the cluster −2 rather than +2. This affectively prevented strong interactions between the linker and GAGs. Besides the changes in the linker, N40/B356 strains of DBPA are also devoid of residues equivalent to B31's K124 and K128. However, these residues are not located in the binding pocket and have not been perturbed significantly in either chemical shift mapping or the PRE experiments, thus may not play a significant role in GAG binding. The fact that DBPA from strain 297 has strong affinity for GAGs despite not having a residue equivalent to K128 also partially confirms the hypothesis. The differences in GAG binding affinity between B31 and N40 DBPAs cannot be attributed to lack of basic amino acids in N40 DBPA either: N40 has a comparable number of basic amino acids in its version of DBPA as B31 (27 basic amino acids in N40 vs. 29 in B31) as well as similar basic-to-acidic residue ratios as B31 (1.08 vs 1.07). Therefore, the lack of the BXBB motif could be a major factor in N40 DBPA's lower GAG affinity. In fact, this variation in DBPA sequence could be a significant contributing factor to the observed lower binding efficiency to host cells by the N40 strains of Borrelia (38). An analysis of all DBPA sequences from Borrelia burgdorferi available in the UniProt database showed that out of 20 sequences available, 7 possessed the BXBB motif, indicating the GAG-binding enhancing epitope is not exclusive to strains B31 and 297.

In this report, the role played by the BXBB motif in GAG binding has been experimentally verified using paramagnetically tagged GAG ligands. In addition to providing confirmation of interactions between the BXBB motif and GAGs, results from the titration of DBPA by the paramagnetic ligand are surprising in that it shows DBPA's interaction with GAGs maybe highly orientation specific. The fact that only residues in the linkers experienced significant PRE indicates the reducing end of the ligand is close to the linker. However, the C-terminus, which is located at the opposite side of the binding pocket, may not be. An

alternative explanation is that the C-terminus's affinity for GAGs is weaker, therefore may not be affected by PRE to the same extent as the linker residues when the reducing end is close to it. Consequently, the binding mode with the fragment in the opposite orientation may not be detected by PRE. It is also unclear whether the specificity is the consequence of the opening of the reducing end monosaccharide during reductive amination. The increased flexibility due to the linearization of the sugar may have artificially increased the pockets affinity for the reducing end. However, if the observation is not the result of an artifact, it shows DBPA's interactions with GAGs are highly specific and maybe the result of close geometric matching between sulfate groups on GAGs and basic amino acids in DBPA.

Characterization of the DBPA's backbone dynamics showed conformational entropy does not appear to be a significant factor in determining the binding affinity. This agrees with the small entropic change measured in ITC. The fact that one of the most flexible segments of the protein also contains a crucial GAG binding epitope is demonstrative of the dynamic nature of DBPA-GAG interactions and lends a plausible explanation to the weak interaction DBPA has with GAGs. However, despite the millimolar dissociation constants for these interactions, the interaction is by no means irrelevant. The dissociation constants measured in this study pertain to only low molecular weight heparin fragments. However, it is well known that the affinity of proteins for GAGs is highly dependent on the size of GAGs. Longer GAG polymers in vivo will have a much higher affinity for DBPA than the hexasaccharide used in this study due to the effects of avidity. This does not imply the use of short GAG fragments as the ligand is not relevant. The size of GAG-binding pocket on DBPA can only accommodate one hexasaccharide at a time; therefore hexasaccharides are the right size to achieve sufficient affinity without the risk of promoting protein oligomerization. Size-defined GAG fragments also allowed for a more objective evaluation of DBPA's preferences for different GAG types. In fact, such weak interactions are by no means extra-ordinary in protein-carbohydrate interactions(39). Specifically, the well studied interactions between influenza A viral hemagglutinin monomer and its sialyated N-glycan receptor possess dissociation constants in the millimolar range,(40) as does the interaction between high mannose N-glycan and the immune receptor DC-SIGN (41). These weak interactions are still relevant because most protein-carbohydrate interactions rely on multivalency and avidity effects to achieve sufficient binding affinity. Both factors should play a role in DBPA-mediated interactions with GAGs.

Although the GAG-binding site composed of the linker residues and the C-terminus is the highest affinity site on DBPA, titrations with conventional GAG ligands have also revealed that the N-terminus maybe a weaker secondary binding site. These interactions are manifested in the significant chemical shift changes in atoms from N-terminal residues T28 and T101 during heparin dp6 titrations (figure 3). However, K_D fitting showed that the dissociation constant of the binding is much weaker than residues located in the high affinity site (3 mM vs. 0.5 mM, supplementary figure 9), and mutations at the main site left the K_D at the N-terminal site unchanged, indicating the N-terminal site is independent from the main GAG binding site. The catalyst of these interactions is most likely a cluster of basic amino acids at the N-terminus including R34, K102 and K104. The helical conformation of the segment allowed them to form a basic strip at the N-terminus that offers optimal geometry to interact with GAGs. HSQCs of Arg sidechain Hε-Nε showed the side chain of R34 experienced significant changes in chemical shifts and signal intensity in the presence of heparin dp6 fragments (data not shown). This provides further proof that the N-terminus is involved in GAG-binding. Although of weaker affinity than the main GAG-binding site, the secondary binding site may still offer significant contributions to DBPA's interactions with native GAG polymers in vivo.

Supplementary Material

Refer to Web version on PubMed Central for supplementary material.

Acknowledgments

Funding Source: This research is supported by a grant from the National Institute of General Medical Sciences' K99/R00 program (5R00GM088483) and funds from Arizona State University.

We thank Dr. Brian Cherry for the maintenance of spectrometers and Dr. Andrey Bobokov of Sanford-Burnham Medical Research Institute for performing the ITC titrations. This research is supported by grants from the National Institute of General Medical Sciences K99/R00 program (5R00GM088483) and funds from Arizona State University.

ABBREVIATIONS

DBP	Decorin binding protein
DBPA	Decorin binding protein A
DBPB	Decorin binding protein B
GAG	Glycosaminoglycan
GMSA	Gel mobility shift assay
ITC	Isothermal titration calorimetry
HSQC	Heteronuclear single quantum coherence
PRE	Paramagnetic Relaxation Enhancement
SAX	Strong anion exchange
SDS-PAGE	Sodium dodecyl sulfate polyacrylamide gel electrophoresis

References

1. Krupka M, Zachova K, Weigl E, Raska M. Prevention of Lyme Disease: Promising Research or Sisyphean Task? Arch Immunol Ther Exp. 2011; 59:261–275.
2. Fallon BA, Levin ES, Schweitzer PJ, Hardesty D. Inflammation and central nervous system Lyme disease. Neurobiol Dis. 2010; 37:534–541. [PubMed: 19944760]
3. Halperin JJ. Nervous system Lyme disease. J Neurol Sci. 1998; 153:182–191. [PubMed: 9511877]
4. Schuijt TJ, Hovius JW, van der Poll T, van Dam AP, Fikrig E. Lyme borreliosis vaccination: the facts, the challenge, the future. Trends Parasitol. 2011; 27:40–47. [PubMed: 20594913]
5. Guo BP, Brown EL, Dorward DW, Rosenberg LC, Hook M. Decorin-binding adhesins from Borrelia burgdorferi. Molecular microbiology. 1998; 30:711–723. [PubMed: 10094620]
6. Guo BP, Norris SJ, Rosenberg LC, Hook M. Adherence of Borrelia burgdorferi to the proteoglycan decorin. Infection and immunity. 1995; 63:3467–3472. [PubMed: 7642279]
7. Leong JM, Wang H, Magoun L, Field JA, Morrissey PE, Robbins D, Tatro JB, Coburn J, Parveen N. Different classes of proteoglycans contribute to the attachment of Borrelia burgdorferi to cultured endothelial and brain cells. Infection and immunity. 1998; 66:994–999. [PubMed: 9488387]
8. Parveen N, Robbins D, Leong JM. Strain variation in glycosaminoglycan recognition influences cell-type-specific binding by lyme disease spirochetes. Infect Immun. 1999; 67:1743–1749. [PubMed: 10085013]
9. Brown EL, Wooten RM, Johnson BJ, Iozzo RV, Smith A, Dolan MC, Guo BP, Weis JJ, Hook M. Resistance to Lyme disease in decorin-deficient mice. J Clin Invest. 2001; 107:845–852. [PubMed: 11285303]

10. Shi Y, Xu Q, McShan K, Liang FT. Both decorin-binding proteins A and B are critical for the overall virulence of Borrelia burgdorferi. Infection and immunity. 2008; 76:1239–1246. [PubMed: 18195034]
11. Weening EH, Parveen N, Trzeciakowski JP, Leong JM, Hoeoek M, Skare JT. Borrelia burgdorferi Lacking DbpBA Exhibits an Early Survival Defect during Experimental Infection. Infection and immunity. 2008; 76:5694–5705. [PubMed: 18809667]
12. Blevins JS, Hagman KE, Norgard MV. Assessment of decorin-binding protein A to the infectivity of Borrelia burgdorferi in the murine models of needle and tick infection. BMC Microbiol. 2008; 8
13. Shi Y, Xu Q, Seemanaplli SV, McShan K, Liang FT. Common and unique contributions of decorin-binding proteins A and B to the overall virulence of Borrelia burgdorferi. PloS one. 2008; 3:e3340. [PubMed: 18833332]
14. Fischer JR, Parveen N, Magoun L, Leong JM. Decorin-binding proteins A and B confer distinct mammalian cell type-specific attachment by Borrelia burgdorferi, the Lyme disease spirochete. Proceedings of the National Academy of Sciences of the United States of America. 2003; 100:7307–7312. [PubMed: 12773620]
15. Parveen N, Caimano M, Radolf JD, Leong JM. Adaptation of the Lyme disease spirochaete to the mammalian host environment results in enhanced glycosaminoglycan and host cell binding. Molecular microbiology. 2003; 47:1433–1444. [PubMed: 12603746]
16. Benoit VM, Fischer JR, Lin YP, Parveen N, Leong JM. Allelic variation of the Lyme disease spirochete adhesin DbpA influences spirochetal binding to decorin, dermatan sulfate, and mammalian cells. Infection and immunity. 2011; 79:3501–3509. [PubMed: 21708995]
17. Wang X. Solution structure of decorin-binding protein A from *Borrelia burgdorferi*. Biochem J. 2012; 51:8353–8362.
18. Leong JM, Robbins D, Rosenfeld L, Lahiri B, Parveen N. Structural requirements for glycosaminoglycan recognition by the Lyme disease spirochete, Borrelia burgdorferi. Infection and immunity. 1998; 66:6045–6048. [PubMed: 9826395]
19. Brown EL, Guo BP, O'Neal P, Hook M. Adherence of Borrelia burgdorferi. Identification of critical lysine residues in DbpA required for decorin binding. The Journal of biological chemistry. 1999; 274:26272–26278. [PubMed: 10473582]
20. Wang X. Solution structure of decorin-binding protein A from Borrelia burgdorferi. Biochemistry. 2012; 51:8353–8362. [PubMed: 22985470]
21. Catanzariti AM, Soboleva TA, Jans DA, Board PG, Baker RT. An efficient system for high-level expression and easy purification of authentic recombinant proteins. Protein Science. 2004; 13:1331–1339. [PubMed: 15096636]
22. Xiao Z, Zhao W, Yang B, Zhang Z, Guan H, Linhardt RJ. Heparinase 1 selectivity for the 3,6-di-O-sulfo-2-deoxy-2-sulfamido-alpha-D-glucopyranose (1,4) 2-O-sulfo-alpha-L-idopyranosyluronic acid (GlcNS3S6S-IdoA2S) linkages. Glycobiology. 2011; 21:13–22. [PubMed: 20729345]
23. Lyon M, Deakin JA, Lietha D, Gherardi E, Gallagher JT. The Interactions of Hepatocyte Growth Factor/Scatter Factor and Its NK1 and NK2 Variants with Glycosaminoglycans Using a Modified Gel Mobility Shift Assay. Journal of Biological Chemistry. 2004; 279:43560–43567. [PubMed: 15292253]
24. Seo ES, Blaum BS, Vargues T, De Cecco M, Deakin JA, Lyon M, Barran PE, Campopiano DJ, Uhrin D. Interaction of human beta-defensin 2 (HBD2) with glycosaminoglycans. Biochemistry. 2010; 49:10486–10495. [PubMed: 21062008]
25. Farmer BT 2nd, Constantine KL, Goldfarb V, Friedrichs MS, Wittekind M, Yanchunas J Jr, Robertson JG, Mueller L. Localizing the NADP+ binding site on the MurB enzyme by NMR. Nat Struct Biol. 1996; 3:995–997. [PubMed: 8946851]
26. Iwahara J, Tang C, Marius Clore G. Practical aspects of (1)H transverse paramagnetic relaxation enhancement measurements on macromolecules. J Magn Reson. 2007; 184:185–195. [PubMed: 17084097]
27. Delaglio F, Grzesiek S, Vuister GW, Zhu G, Pfeifer J, Bax A. Nmrpipe - a Multidimensional Spectral Processing System Based on Unix Pipes. J Biomol Nmr. 1995; 6:277–293. [PubMed: 8520220]

28. Johnson BA. Using NMRView to visualize and analyze the NMR spectra of macromolecules. Methods Mol Biol. 2004; 278:313–352. [PubMed: 15318002]
29. d'Auvergne EJ, Gooley PR. Optimisation of NMR dynamic models I. Minimisation algorithms and their performance within the model-free and Brownian rotational diffusion spaces. J Biomol Nmr. 2008; 40:107–119. [PubMed: 18085410]
30. Kay LE, Torchia DA, Bax A. Backbone dynamics of proteins as studied by 15N inverse detected heteronuclear NMR spectroscopy: application to staphylococcal nuclease. Biochemistry. 1989; 28:8972–8979. [PubMed: 2690953]
31. Pikas DS, Brown EL, Gurusiddappa S, Lee LY, Xu Y, Hook M. Decorin-binding sites in the adhesin DbpA from Borrelia burgdorferi: a synthetic peptide approach. The Journal of biological chemistry. 2003; 278:30920–30926. [PubMed: 12761224]
32. Lis H, Sharon N. Lectins: Carbohydrate-Specific Proteins That Mediate Cellular Recognition. Chem Rev. 1998; 98:637–674. [PubMed: 11848911]
33. Gemma E, Hulme AN, Jahnke A, Jin L, Lyon M, Muller RM, Uhrin D. DMT-MM mediated functionalisation of the non-reducing end of glycosaminoglycans. Chem Commun (Camb). 2007:2686–2688. [PubMed: 17594020]
34. Jain NU, Venot A, Umemoto K, Leffler H, Prestegard JH. Distance mapping of protein-binding sites using spin-labeled oligosaccharide ligands. Protein Sci. 2001; 10:2393–2400. [PubMed: 11604544]
35. Lipari G, Szabo A. Model-Free Approach to the Interpretation of Nuclear Magnetic Resonance Relaxation in Macromolecules. 1. Theory and Range of Validity. J Am Chem Soc. 1982; 104:4546–4559.
36. Lipari G, Szabo A. Model-Free Approach to the Interpretation of Nuclear Magnetic Resonance Relaxation in Macromolecules. 2. Analysis of Experimental Results. J Am Chem Soc. 1982; 104:4559–4570.
37. Imai DM, Samuels DS, Feng S, Hodzic E, Olsen K, Barthold SW. The early dissemination defect attributed to disruption of decorin-binding proteins is abolished in chronic murine lyme borreliosis. Infect Immun. 2013; 81:1663–1673. [PubMed: 23460518]
38. Chan K, Awan M, Barthold SW, Parveen N. Comparative molecular analyses of Borrelia burgdorferi sensu stricto strains B31 and N40D10/E9 and determination of their pathogenicity. BMC Microbiol. 2012; 12:157. [PubMed: 22846633]
39. Varki, A. Essentials of glycobiology. 2. Cold Spring Harbor Laboratory Press; Cold Spring Harbor, N.Y: 2009.
40. Takemoto DK, Skehel JJ, Wiley DC. A surface plasmon resonance assay for the binding of influenza virus hemagglutinin to its sialic acid receptor. Virology. 1996; 217:452–458. [PubMed: 8610436]
41. Probert F, Whittaker SB, Crispin M, Mitchell DA, Dixon AM. Solution NMR Analyses of the C-type Carbohydrate Recognition Domain of DC-SIGNR Protein Reveal Different Binding Modes for HIV-derived Oligosaccharides and Smaller Glycan Fragments. J Biol Chem. 2013; 288:22745–22757. [PubMed: 23788638]

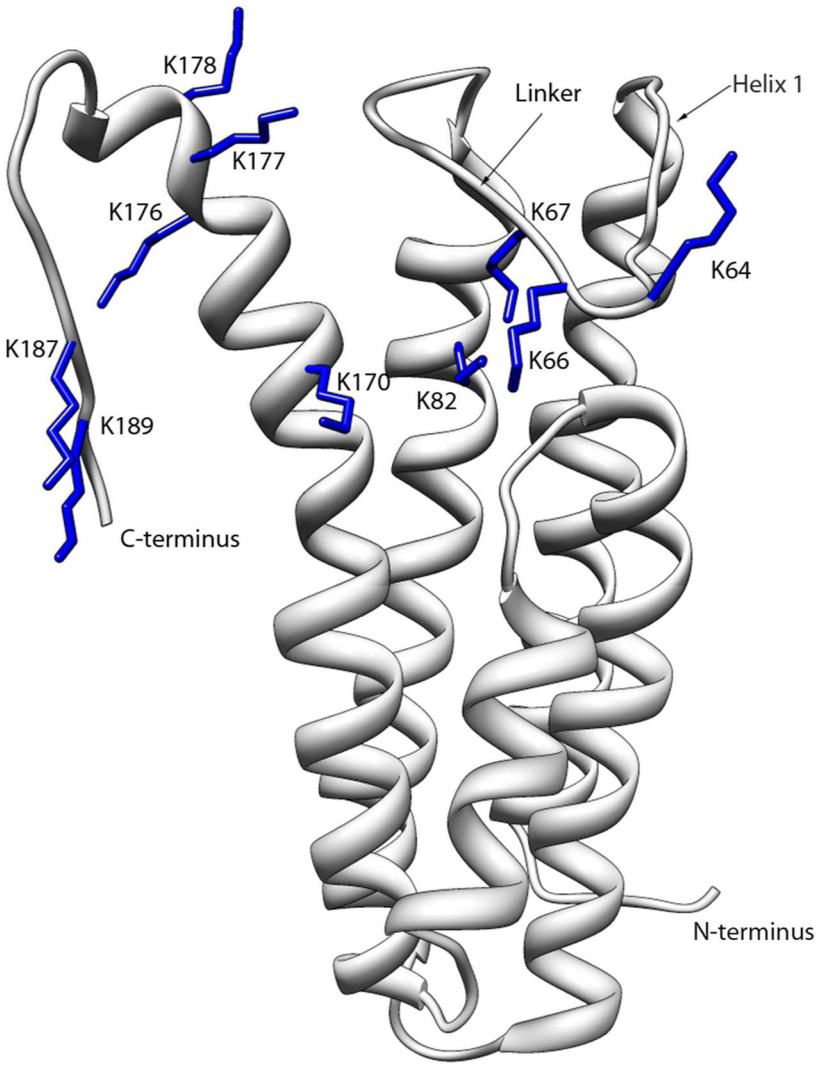

Figure 1.
Ribbon depiction of DBPA B31 WT with the side chains of the lysine residues mutated colored blue.

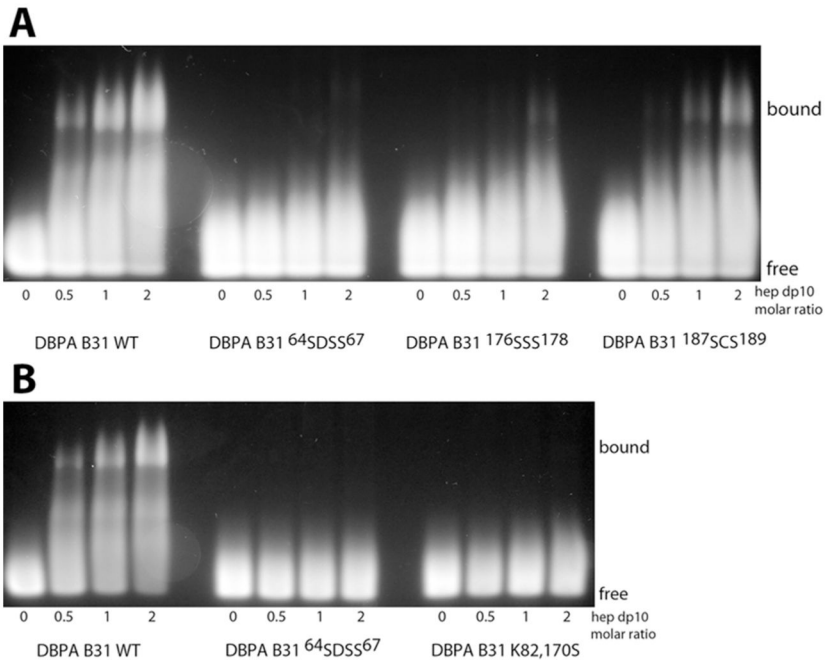

Figure 2.

Gel mobility shift assay of heparin dp10 in the presence of increasing concentrations of (A) B31 WT, ^{64}SDSS^{67}, ^{176}SSS^{178}, and ^{187}SCS^{189} and of (B) B31 WT, ^{64}SDSS^{67}, and K82,170S.

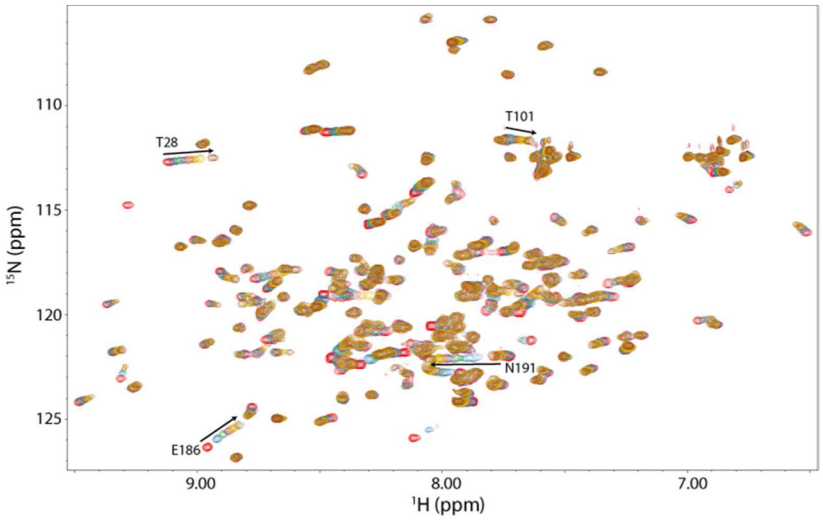

Figure 3.

^{1}H—^{15}N HSQC overlays of DBPA B31 WT in the presence of increasing concentrations of heparin dp6. Signals experiencing a large migration (E186 and N191) are indicated with the residue number and direction of migration. The red contour represents the initial HSQC spectrum of DBPA in the absence of heparin dp6. Each subsequently colored contour represents the HSQC spectrum of DBPA at different concentrations of heparin dp6. The concentrations of heparin dp6 are 0.3, 0.6, 0.9, 1.2, 1.5, and 2.4 mM. The concentration of DPBA is 0.15 mM.

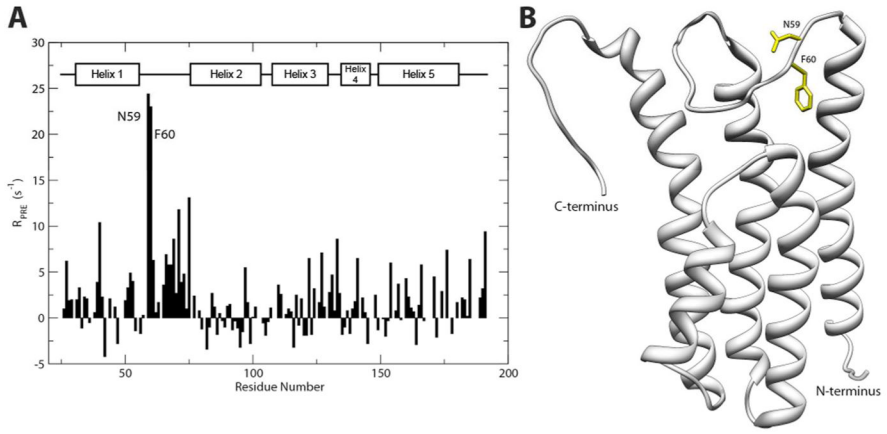

Figure 4.

(A) Comparison of residue-specific PRE effect on the backbone amide proton from TEMPO-labeled heparin dp6 before and after reduction of the TEMPO radical. The comparison indicated that two residues (N59 and F60) experienced a greater PRE effect when probed with the TEMPO radical. (B) Ribbon depiction of DBPA B31 WT with the residues experiencing the greatest PRE effect colored yellow.

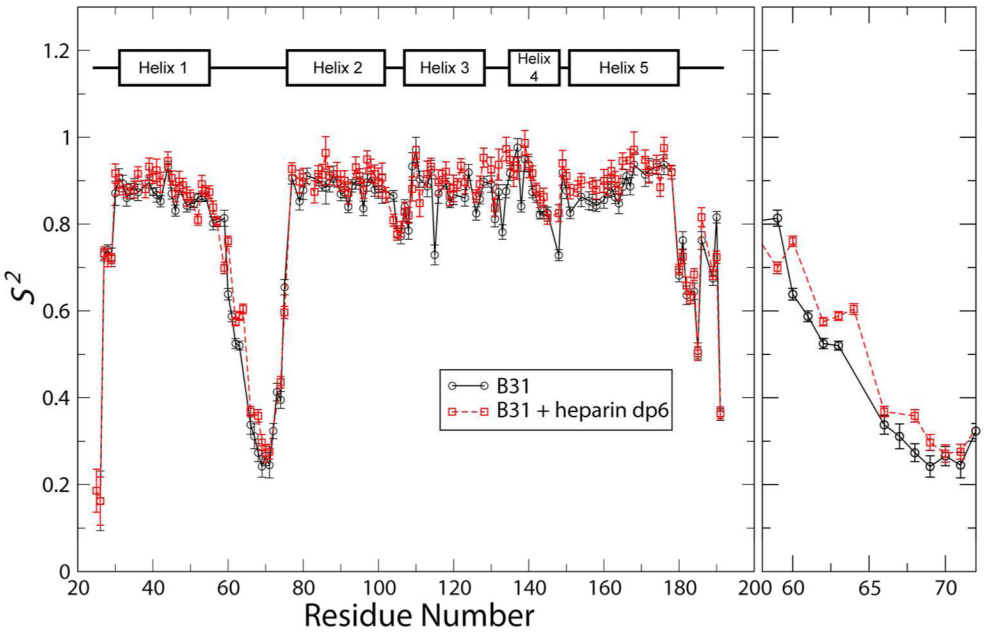

Figure 5.
Order parameter of backbone amide nitrogen atoms for DBPA B31 WT in the absence (—) and presence (- -) of 24 molar equivalents of heparin dp6. Details of order parameter changes for residues in the first half of the flexible linker are shown in the right panel.

Table 1

K_D of DBPA-heparin dp6 interaction from calculation using chemical shift changes from residues E186 and N191 of DBPA B31 variants as well as from ITC.

B31 Mutant	K_D (mM)		
	N191	E186	ITC
WT	0.55 ± 0.04	0.76 ± 0.04	0.75 ± 0.03
^{64}SDSS^{67}	> 20	> 50	~ 5.2 ± 0.8
K82,170S	4 ± 1	—	~ 11 ± 3
^{176}SSS^{178}	2.5 ± 0.5	3.3 ± 0.7	—
^{187}SCS^{189}	0.85 ± 0.06	2.0 ± 0.3	—